

## Supporting Information

### Cationic Groups in Polystyrene/O-PBI Blends influence Performance and Hydrogen Crossover in AEMWE

Linus Hager,\* Maximilian Schrodtt, Manuel Hegelheimer, Julian Stonawski, Pradipkumar Leuaa, Christodoulos Chatzichristodoulou, Andreas Hutzler, Thomas Böhm, Simon Thiele and Jochen Kerres\*

\*Corresponding authors

#### Materials:

The polybenzimidazole O-PBI with a number/mass average molecular weight of  $M_n/M_w = 170/339 \text{ kg mol}^{-1}$  was obtained from FUMATECH BWT GmbH. PiperION®(60  $\mu\text{m}$ , self-supporting) was obtained from fuelcellstore. 4-chlorostyrene was purchased from Manchester Organics. Magnesium, tetrahydrofuran (dry), dimethylacetamide (DMAc), 1,2-dibromoethane, 1,6-dibromohexane, lithium bromide, copper(I) bromide, diethyl ether, 2,2'-azobis(2-methylpropionitrile) (AIBN), dimethylformamide, dimethyl sulfoxide, acetonitrile, sodium tungstate,  $\text{Ni}(\text{NO}_3)_2 \cdot 6\text{H}_2\text{O}$ , Urea, quinuclidine and magnesium sulfate were purchased from Sigma Aldrich and used without further purification. KOH (ACS reagent., >85% KOH basis, pellets, Fluka) was procured from Sigma Aldrich. 1-methylpiperidine,  $\text{Fe}(\text{NO}_3)_3 \cdot 9\text{H}_2\text{O}$ , trimethyl amine (4.2 M in ethanol), and ammonium fluoride were obtained from Thermo Fisher Scientific and used without further purification.

#### Monomer synthesis:

**Synthesis of 4-(6-bromohexyl) styrene:** Under an argon atmosphere, Mg (16.750 g, 0.6890 mol, 1.06 eq.) was added to a three-neck round bottom flask. Subsequently, 4-Chlorostyrene (87 mL, 0.75 M in THF) was added. The mixture was heated to reflux, and a few drops of 1,2-dibromoethane were added to start the reaction. While keeping the reaction mixture under reflux, the remaining 4-Chlorostyrene (780 mL, 0.75 M in THF) was added dropwise within 1 h. After stirring for 90 min under reflux, the reaction was allowed to cool to room temperature and stirred for another hour. After that, the Grignard solution obtained was used without further purification or analysis. LiBr (7.817 g, 90.00 mmol) and CuBr (6.455 g, 45.00 mmol) were dissolved in dry THF (90 mL) to form the active catalyst ( $\text{LiCuBr}_2$ ). The  $\text{LiCuBr}_2$  solution (80 mL) was added to a solution of 1,6-dibromohexane (1.586 kg, 6.500 mol, 10.0 eq.) in dry THF (1300 mL) and cooled to 0°C. The styryl Grignard was added slowly to the ice-cooled 1,6-dibromohexane solution over 2 h. Afterward, the solution was stirred at room temperature for 16 h and then quenched by the addition of NaCN (52.00 g, 1.061 mol) and  $\text{NH}_4\text{Cl}$  (325.0 g, 6.075 mol) dissolved in ultrapure water (1.000 L). The aqueous phase was extracted twice with diethyl ether (1.5 L), and the combined organic phases were washed twice with ultrapure water (1.000 L). Diethyl ether was removed under reduced pressure after the combined organic phases were dried over  $\text{MgSO}_4$ . The residual 1,6-dibromohexane was removed by vacuum distillation. Tert-butyl catechol (4.000 g) was added to prevent spontaneous polymerization during the distillation. The crude product was purified by vacuum distillation ( $T_{\text{vapor}} = 100\text{-}110^\circ\text{C}$ ,  $p = 0.001 \text{ mbar}$ ) to obtain the pure product as a colorless oil—yield: 109.40 g (63 %).  $^1\text{H NMR}$  (500 MHz,  $\text{CHCl}_3\text{-d}$ ,  $\delta$ ): 7.34 (d,  $J = 8.2 \text{ Hz}$ , 2H; Ar H), 7.14 (d,  $J = 8.2 \text{ Hz}$ , 2H; Ar H), 6.72 (dd,  $J = 17.6, 10.9 \text{ Hz}$ , 1H;  $\text{CH}=\text{CH}_2$ ), 5.72 (d,  $J = 17.6 \text{ Hz}$ , 1H;  $\text{CH}=\text{CH}_2$ ), 5.20 (d,  $J = 10.9 \text{ Hz}$ , 1H;  $\text{CH}=\text{CH}_2$ ), 3.42 (t,  $J = 6.8 \text{ Hz}$ , 2H;  $\text{CH}_2\text{-Br}$ ), 2.62 (t,  $J = 7.7 \text{ Hz}$ , 2H;  $\text{CH}_2\text{-Ar}$ ), 1.89 (m, 2H,  $\text{CH}_2\text{-CH}_2\text{-Br}$ ), 1.66 (m, 2H,  $\text{CH}_2\text{-CH}_2\text{-Ar}$ ), 1.50-1.45 (m, 2H,  $\text{CH}_2\text{-CH}_2\text{-CH}_2\text{-Br}$ ), 1.39-1.34 (m, 2H,  $\text{CH}_2\text{-CH}_2\text{-CH}_2\text{-Ar}$ ).  $^{13}\text{C NMR}$  (125 MHz,  $\text{CHCl}_3\text{-d}$ ,  $\delta$ ): 142.5 ( $\text{C}_{\text{ar}}\text{-CH}_2$ ), 136.8

(CH=CH<sub>2</sub>), 135.3 (C<sub>ar</sub>-CH=CH<sub>2</sub>), 128.7 (C<sub>ar</sub>-C<sub>ar</sub>-CH<sub>2</sub>), 128.7 (C<sub>ar</sub>-C<sub>ar</sub>-CH<sub>2</sub>), 126.3 (C<sub>ar</sub>-C<sub>ar</sub>-CH=CH<sub>2</sub>), 126.3 (C<sub>ar</sub>-C<sub>ar</sub>-CH=CH<sub>2</sub>), 113.0 (CH<sub>2</sub>=CH), 35.6 (CH<sub>2</sub>-C<sub>ar</sub>), 34.1 (CH<sub>2</sub>-Br), 32.8 (CH<sub>2</sub>-CH<sub>2</sub>-Br), 31.3 (CH<sub>2</sub>-CH<sub>2</sub>-C<sub>ar</sub>), 28.5 (CH<sub>2</sub>-CH<sub>2</sub>-CH<sub>2</sub>-Br), 28.1 (CH<sub>2</sub>-CH<sub>2</sub>-CH<sub>2</sub>-C<sub>ar</sub>).

**Synthesis of 1-butyl-2-mesityl-4,5-dimethyl-1H-imidazole:** The synthesis was performed with a slightly adapted literature procedure.<sup>1</sup> Diacetyl (14.463 g, 168.00 mmol, 1.000 eq.) and 2,4,6-trimethylbenzaldehyde (25.00 mL, 168.00 mmol, 1.00 eq.) were dissolved in methanol. Afterward, ammonium acetate (12.936 g, 168.00 mmol, 1.000 eq.), n-butylamine (16.605 mL, 168.00 mmol, 1.00 eq.) and L-proline (2.940 g, 25.536 mmol, 0.152 eq.) were added and the reaction mixture was stirred under reflux overnight. After cooling to room temperature, the solvent was removed under reduced pressure. The residue was dissolved in chloroform (150 mL) and washed with H<sub>2</sub>O twice. The combined organic phases were dried over MgSO<sub>4</sub> and filtered. The solvent was removed under reduced pressure. The crude mixture was purified via flash column chromatography (methanol/dichloromethane 5:95 vol/vol% to methanol/dichloromethane 50:50 vol/vol%) to afford a brown oil. Finally, the crude product was again purified further flash column chromatography (ethyl acetate/cyclohexane 5:95 vol/vol % to ethyl acetate 100 vol%) to give 1-butyl-2-mesityl-4,5-dimethyl-1H-imidazole as a pale brown, soft crystalline solid.

<sup>1</sup>H NMR (500 MHz, CHCl<sub>3</sub>-d, δ): δ 6.86 (s, 2H, H<sub>Ar</sub>), 3.46 (m, 2H, N-CH<sub>2</sub>), 2.29 (s, 3H, para-CH<sub>3</sub>-Ar), 2.19 (s, 3H, CH<sub>3</sub>-C-N), 2.18 (s, 3H, CH<sub>3</sub>-C-N), 2.01 (s, 3H, ortho-CH<sub>3</sub>-Ar), 1.40 (m, 2H, N-CH<sub>2</sub>-CH<sub>2</sub>) 1.12 (sext, J = 7.4 Hz, 2H, N-CH<sub>2</sub>-CH<sub>2</sub>-CH<sub>2</sub>), 0.77-0.80 (t, J = 7.4 Hz, CH<sub>2</sub>-CH<sub>3</sub>).

### Polymerization:

4-(6-Bromohexyl)styrene (20.290 g, 75.930 mmol, 1 eq) was destabilized by passing it through a short column of basic alumina (alox) and subsequently dissolved in chlorobenzene (75 mL). AIBN (0.200 g, 1.220 mmol, 0.016 eq) was added, and the mixture was degassed with Ar for 15 min. The mixture was stirred at 65°C for 16 h. Afterward, the mixture was precipitated in MeOH, redissolved in THF, and again precipitated in MeOH. The polymer was dried at 85°C overnight. The product was obtained as a colorless rubber —yield: 15.220 g (75 %) <sup>1</sup>H NMR (500 MHz, CHCl<sub>3</sub>-d, δ): 6.56 (m, 4H), 3.38 (m, 2H), 2.51 (m, 2H), 1.56 (m, 12H).

GPC (Polystyrene standards, 35°C, THF): M<sub>n</sub>: 53 700 g mol<sup>-1</sup>, Đ = 2.06

### Quaternization reactions:

P4 was synthesized according to our previously published procedure.<sup>2</sup>

Quaternization with trimethylamine: The precursor polymer poly(4-(6-bromohexyl)styrene (4.001 g, 15.00 mmol, 1.00 eq.) was dissolved in DMAc (140 mL) by stirring at 50°C. Afterward, TMA (36 mL, 150.0 mmol, 4.2 M in ethanol, 10.00 eq.) was added to the solution. The reaction mixture was stirred at 50°C for 48 h. After cooling to room temperature, the polymer was purified by dialysis against absolute ethanol and subsequently dried under a vacuum.

Quaternization with quinuclidine: The precursor polymer poly(4-(6-bromohexyl)styrene (4.001 g, 15.00 mmol, 1.00 eq.) was dissolved in DMAc (140 mL) by stirring at 50°C. Afterward, quinuclidine (2.502 g, 22.50 mmol, 1.50 eq.) was added to the solution. The reaction mixture was stirred at 50°C for 48 h. After cooling to room temperature, the polymer was purified by dialysis against absolute ethanol and subsequently dried under a vacuum.

Quaternization with 1-butyl-2-mesityl-4,5-dimethyl-1H-imidazole: The precursor polymer poly(4-(6-bromohexyl)styrene (2.138 g, 8.000 mmol, 1.00 eq.) was dissolved in DMAc (74 mL) by stirring at 50°C. Afterward, 1-butyl-2-mesityl-4,5-dimethyl-1H-imidazole (3.245 g, 12.00 mmol, 1.50 eq.) was added to the solution. The

reaction mixture was stirred at 120°C for 48 h. After cooling to room temperature, the polymer was purified by dialysis against absolute ethanol and subsequently dried under a vacuum.

### Membrane preparation:

The blend membrane preparation is exemplarily described for M3. 1200 mg of P3 was dissolved in DMSO (15.7 g) by stirring at 60°C. Afterward, the O-PBI solution (5wt% in DMSO, 6.892 g) was added, and the solution was homogenized by stirring at 80°C for 1 d. The membrane was cast with a doctor blade (gap width: 1400 mm) and dried at 70°C on the doctor blade for 2 h. Afterward, the remaining solvent was evaporated in a ventilation oven at 80°C for 4 h. The membrane was placed in 1 M HCL for 1 d at 85 °. Afterward, the membrane was fully converted into chloride form by immersion of the membrane in 1 M NaCl<sub>aq</sub> for 1 d. The membrane was washed with ultrapure water for 1 d at 85 ° and dried at 85°C overnight. The other blend membranes were prepared accordingly.

### Polymer and membrane characterization:

**Nuclear Magnetic Resonance:** NMR spectra were measured at room temperature with a JEOL JNM-ECZ-500R with a proton resonance frequency of 500 MHz. For the different NMR measurements, samples were dissolved in deuterated chloroform (CHCl<sub>3</sub>-d) deuterated dimethyl sulfoxide (DMSO-d<sub>6</sub>). The signal of the residual protons in the deuterated solvent was selected as the internal standard with a shift of 7.26 ppm for CHCl<sub>3</sub>-d and 2.50 ppm for DMSO-d<sub>6</sub>.

**Gel permeation chromatography (GPC):** GPC measurements were performed using a SECcurity2 1260 from PSS. A PSS SDV LUX GUARD was used as a guard column, and three separation columns (2x PSS SDV LUX 3 μm 1000 Å and 1x PSS SDV LUX 3 μm 10000 Å) were applied for sample analysis. The eluent was THF with a 1.0 ml/min flow rate at 35°C. A dual variable wavelength UV-Vis (P/N 404-2107, PSS) and a refractive index detector (P/N 404-2106, PSS) were used as detectors. The relative molecular weight was obtained by calibration with narrowly distributed polystyrene standards from PSS.

**Thermogravimetric analysis (TGA):** The thermal stability of the polymers and membranes was analyzed using a TGA 8000 from PerkinElmer with a heating rate of 20 K min<sup>-1</sup> from 30°C to 800°C under a synthetic air atmosphere.

**Differential Scanning Calorimetry (DSC):** DSC curves were obtained using a Mettler Toledo DSC 3+. Analyses were performed under nitrogen flow (50 mL min<sup>-1</sup>) at a 20 K min<sup>-1</sup> heating rate. The method consisted of three measurement steps with stationary phases of 5 min in between: (1) heating from 0 °C until 250 °C, (2) cooling down to -50 °C, and (3) repeating step 1. The glass transition temperature (T<sub>g</sub>) was calculated using the ISO standard method on the last heating curve.

**Hydroxide Conductivity:** Membrane pieces with the thickness, d, and the width, w, were immersed in degassed 1 M KOH for 24 h to convert the membranes into their mixed hydroxide form. Afterward, the membranes were washed three times with deionized (DI) water to remove excess KOH. The membranes were loaded into an MTS 740 (Scribner Associates) four-point probe conductivity cell. The humidity was controlled at 90 % RH, and the nitrogen flow was at 500 sccm min<sup>-1</sup>. For temperature-dependent measurements, the cell was first equilibrated at 30°C for 1 h, and

then the resistance of the membrane was measured. Then, the temperature was raised by 10°C, and the cell was equilibrated at the respective temperature for 1 h. After equilibration, the resistance was measured again. All measurements were repeated three times. The conductivity was calculated with Equation (1), whereby L is the distance between the two sensing electrodes (l = 0.425 cm), R is the measured resistance, w is the width, and d is the thickness of the membrane:

$$\sigma = \frac{L}{R \cdot w \cdot d} \quad (1)$$

**Mohr's titration and calculation of theoretical IECs:** A membrane in Cl<sup>-</sup> form was immersed in 1 M aqueous NaNO<sub>3</sub> solution for 48 h at room temperature. Afterward, the membrane was withdrawn, and sulfuric acid (250 µL, 2 mol L<sup>-1</sup>) was added to the remaining solution. The solution was titrated at room temperature with 0.01 M aqueous AgNO<sub>3</sub> solution in an OMNIS Titrator with an OMNIS Dosing Module from Metrohm. The IEC was calculated by the following Equation, with V<sub>AgNO<sub>3</sub></sub> as the consumed volume of AgNO<sub>3</sub>, C<sub>AgNO<sub>3</sub></sub> the concentration, and m<sub>dry, OH<sup>-</sup></sub> as the dry mass of the membrane in hydroxide form:

$$IEC_{\text{titrated}} = \frac{V_{\text{AgNO}_3} \cdot C_{\text{AgNO}_3}}{m_{\text{dry, OH}^-}} \quad (2)$$

The theoretical IEC of a blend membrane is given by the weight ratio of the positively charged anion exchange polymer m(P) and O-PBI m(O-PBI). The maximum theoretical IEC is determined by the molecular weight of one repeating unit of the polymer (P) in its hydroxide form:

$$IEC_{\text{theo}} = \frac{m(\text{P, OH}^-)}{M(\text{P, OH}^-) \cdot [(m(\text{P}) + m(\text{OPBI}))]} \quad (3)$$

**Swelling Ratio (SR) and Water Uptake (WU):** A wet piece of the membrane, which previously was immersed in DI water, was gently blotted with lab wipes 7557 provided by KIMTECH®, then weighed, and its thickness, d, was measured with the digital micrometer Series 293 from Mitutoyo. The length, L, was measured with a Garant IP67 caliper gauge. After drying in a vacuum at 60°C for 24 h, the membrane was weighed and measured again. The SR<sub>L</sub>, SR<sub>T</sub>, and WU were calculated with the following formulas:

$$SR_L = \frac{L_{\text{wet}} - L_{\text{dry}}}{m_{\text{dry}}} \cdot 100\% \quad (4)$$

$$SR_T = \frac{d_{\text{wet}} - d_{\text{dry}}}{d_{\text{dry}}} \cdot 100\% \quad (5)$$

$$WU = \frac{m_{\text{wet}} - m_{\text{dry}}}{m_{\text{dry}}} \cdot 100\% \quad (6)$$

The swelling in 1 M KOH was measured accordingly, but 1 M KOH was used instead of DI water.

**Transmission electron microscopy (TEM):** Before TEM analysis, the membranes were immersed in 1 M  $\text{Na}_2\text{WO}_4$  for 72 h, followed by immersion in ultrapure water for 24 h three times each. The  $\text{WO}_4^{2-}$  staining increases the contrast since the image contrast with a high-angle annular dark field (HAADF) detector roughly scales with the square of the atomic number (Rutherford scattering). The membranes were embedded in epoxy resin (Araldite 502) and cut at room temperature with a Diatome ultra 45 diamond knife with water as a floating liquid on an RMC Boeckeler PowerTome. Microstructure analysis was performed using a Talos F200i (ThermoFisher Scientific). The microscope was operated at an acceleration voltage of 200 kV to reduce beam damage. High-angle annular dark field scanning transmission electron microscopy (HAADF-STEM) was utilized to exploit the mass-thickness contrast within ultra-thin sections (100 nm) of the tungstate-stained blend-polymer material. Therefore, a beam current of 47 pA and a convergence angle of 10.5 mrad were adjusted.

**Tensile tests:** The mechanical properties were investigated utilizing an EZ Test EZ-SX from Shimadzu equipped with the SM-100N-168 100 N force transducer from Interface Inc. Seven dry 1.5 cm x 4.0 cm samples were measured for each membrane at a test speed of 10 mm  $\text{min}^{-1}$ . A preload of 0.1 N was applied before the test. The gauge length corresponding to the preload was subtracted from the previously measured gauge length. The Young's Modulus was calculated from a linear fit between 0.05% and 0.25% strain. The tensile strength was set as the stress at the maximum of the stress-strain curve. The measurements were performed at 23°C and 25% RH.

## **AEMWE and hydrogen crossover tests:**

### **Electrode preparation:**

The NiFe-LDH was deposited on the Ni mesh via a hydrothermal synthesis. Therefore, the Ni mesh (Hebei Aegis Metal Materials, 10  $\mu\text{m}$  fiber diameter, 150  $\mu\text{m}$  thickness) was cut to 4.5 cm x 4.5 cm and washed with 1 M HCl, three times DI water, and ethanol in an ultrasonication bath. Afterward, the mesh was dried at room temperature in a vacuum overnight. Then,  $\text{Ni}(\text{NO}_3)_2 \cdot 6\text{H}_2\text{O}$  (0.300 g, 1.032 mmol),  $\text{Fe}(\text{NO}_3)_3 \cdot 9\text{H}_2\text{O}$  (0.140 g, 0.347 mmol),  $\text{NH}_4\text{F}$  (0.040 g, 1.080 mmol) and Urea (0.630 g, 10.490 mmol) were dissolved in 90 mL DI water. The Ni mesh was immersed in the reaction mixture and heated to 120°C for 5 h in an autoclave with a PTFE liner. After cooling to room temperature, the NiFe-LDH functionalized mesh was washed with DI water and ethanol in an ultrasonication bath and dried at 60°C in a ventilation oven.

### **Cell testing:**

The membranes were immersed in 1 M KOH at room temperature overnight. The 1 M KOH electrolyte solution was prepared from KOH pellets and 18.2 M $\Omega$   $\text{cm}^2$  water and pre-electrolyzed at 2.0 V for 24 h with Nickel electrodes to suppress impurities. Before mounting the membranes in the cell, their thicknesses were measured. The cell used for the electrochemical test was made of pure nickel with a pin-type flow field. Before cell setup, the membranes ( $\varnothing=56\text{mm}$ ) and electrodes ( $\varnothing=36\text{mm}$ ) were die-cut into circular pieces and immersed in 1 M KOH for one h. The active area of the cells was 10  $\text{cm}^2$ , with 0.5  $\text{mg cm}^2$  of Pt/C (Tanaka TEC10V40E) and 10 wt% Nafion as binder spray coated (ExactaCoat) on a Freudenberg H23C2 gas diffusion layer (GDL) used as the cathode (thickness = 250  $\mu\text{m}$ ), and NiFe-LDH on a Ni mesh (wire diameter 10  $\mu\text{m}$ , thickness = 150  $\mu\text{m}$ ) from Hebei Aegis Metal Materials as the anode.

PTFE gasket frames with a thickness of 250  $\mu\text{m}$  for the cathode, 150  $\mu\text{m}$  for the anode, and 50  $\mu\text{m}$  for the membrane were used to seal the cell. The cell was fixed with eight M7 screws tightened to a torque of 1 Nm. Heating of the cell was conducted directly in the cell house just behind the flow fields using thermocouples. All tests were performed

at 70°C and ambient pressure. 1 M KOH was circulated through the cell with a flow rate of 60 mL min<sup>-1</sup> in a partially separated mode. The anolyte and catholyte compartments were continuously purged with nitrogen at a flow rate of 57 mL min<sup>-1</sup> and 29 mL min<sup>-1</sup>, respectively. After an initial cell break-in at 1.8 V for 1 h, a galvanostatic controlled polarization curve was recorded (1 mA cm<sup>-2</sup> to 1000 mA cm<sup>-2</sup> with 1 min holding time at each current density), followed by measuring galvanostatic impedance spectroscopy at each current density. Subsequently, hydrogen crossover was evaluated by applying a range of constant current densities, specifically 50, 100, 200, 300, 400, 600, 800, and 1000 mA cm<sup>-2</sup>, and each current density step was maintained for 2 hours. The high cell voltage for M4 limited the crossover measurements to a maximum current density of 800 mA cm<sup>-2</sup>. This constraint was necessary to maintain the voltage below 2.3 V, preventing potential electrode damage. The hydrogen levels in the oxygen stream were measured with an electrochemical hydrogen sensor (Geopal GP-ELK), and sensor calibration was performed before the test using 1%, 0.5%, and 0.1% hydrogen in synthetic air reference. The hydrogen in oxygen level of the last 0.5 h of each current density step was averaged to ensure accuracy, and the data at 100 mA cm<sup>-2</sup> were excluded due to the sensor signal not stabilizing. The exhaust gas from the anode compartment was dried over silica before reaching the hydrogen sensor. Correction of the presented hydrogen crossover data according to the literature was performed.<sup>3,4</sup> The measured hydrogen concentration,  $X_{H_2,meas}$ , represents the molar fraction of hydrogen in the oxygen and the supplied nitrogen ( $\dot{n}_{N_2}$ ). The oxygen production rate,  $\dot{n}_{O_2}$ , was calculated using Faraday's law at each respective current density, assuming 100% Faradaic efficiency for the oxygen evolution reaction (OER) and neglecting any oxygen losses across the membrane. Consequently, the hydrogen crossover flux,  $\Phi_{H_2}$ , was determined according to Equation (7). From the calculated hydrogen flux, the hydrogen concentration in oxygen,  $\Theta_{H_2}$ , was subsequently derived:<sup>4</sup>

$$\Phi_{H_2} = \frac{\dot{n}_{N_2} + \dot{n}_{O_2}}{1 - X_{H_2,meas}} X_{H_2,meas} \quad (7)$$

$$\Theta_{H_2} = \frac{\Phi_{H_2}}{\dot{n}_{O_2} + \Phi_{H_2}} \quad (8)$$

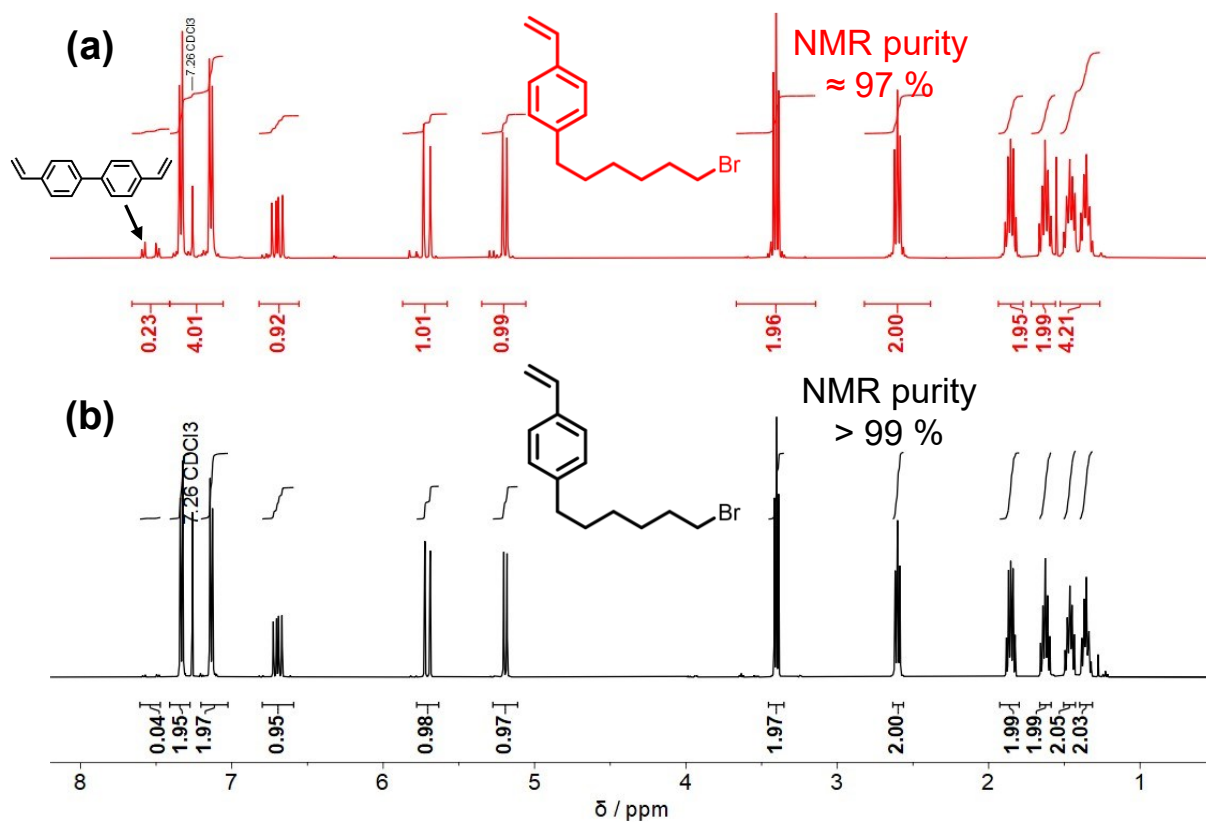


Figure S 1: (a)  $^1\text{H}$  NMR spectra of 4-(6-bromohexyl) styrene synthesized with 4.10 eq. 1,6-dibromohexane and purified by column chromatography with cyclohexane (b)  $^1\text{H}$  NMR spectra of 4-(6-bromohexyl) styrene synthesized with 10.00 eq. 1,6-dibromohexane and purified by vacuum distillation.

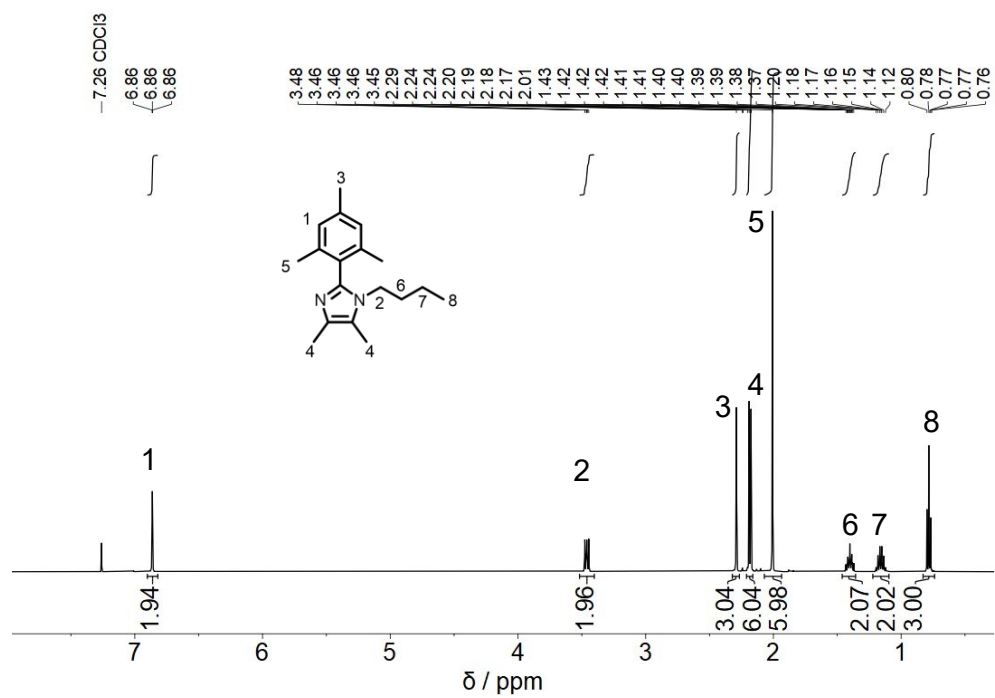


Figure S 2: <sup>1</sup>H-NMR spectrum of 1-butyl-2-mesityl-4,5-dimethyl-1H-imidazole measured in CDCl<sub>3</sub>.



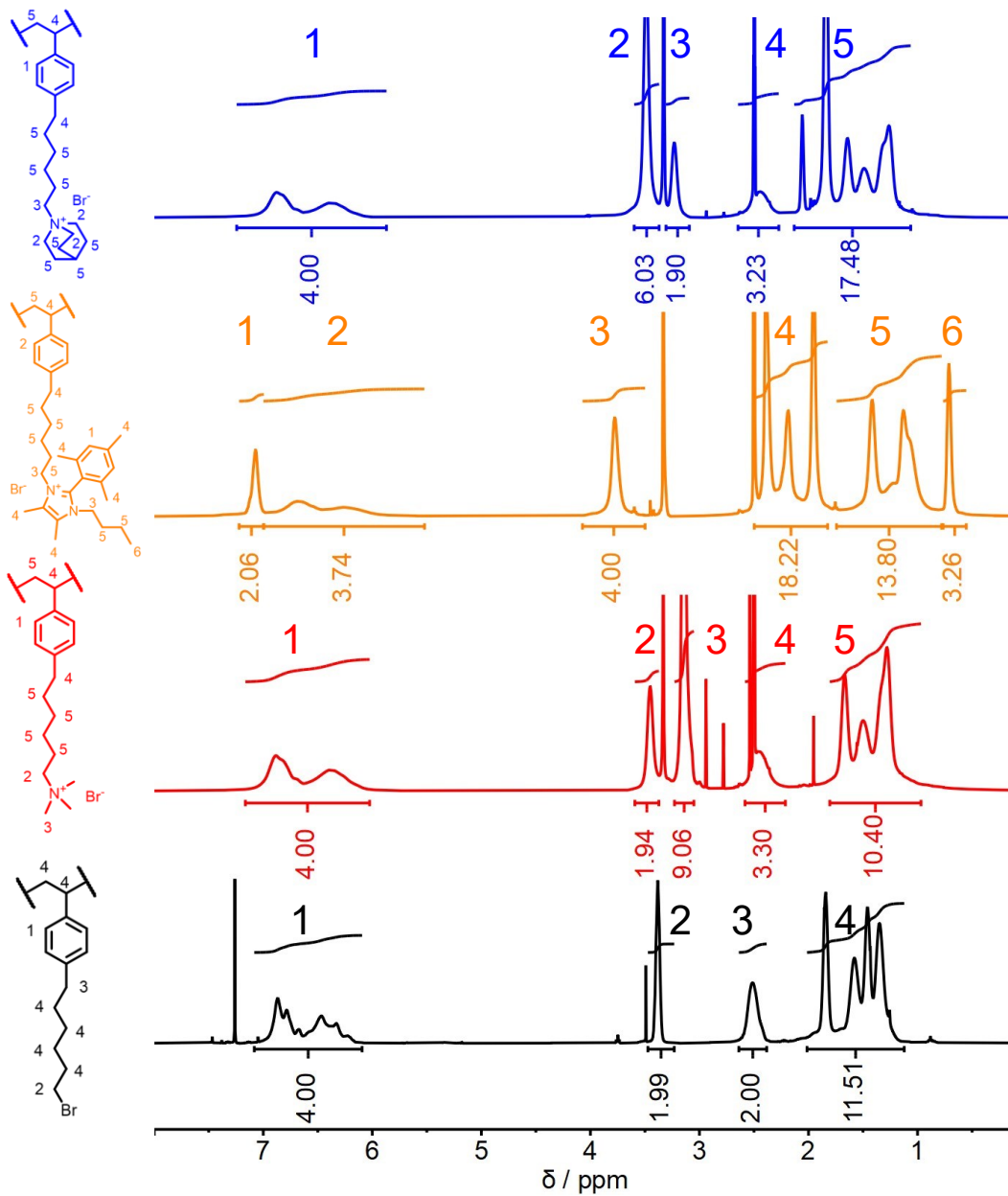


Figure S 3: <sup>1</sup>H NMR spectrum of the precursor polymer and the quaternized polymers with integrated signals and peak assignment to the respective protons.

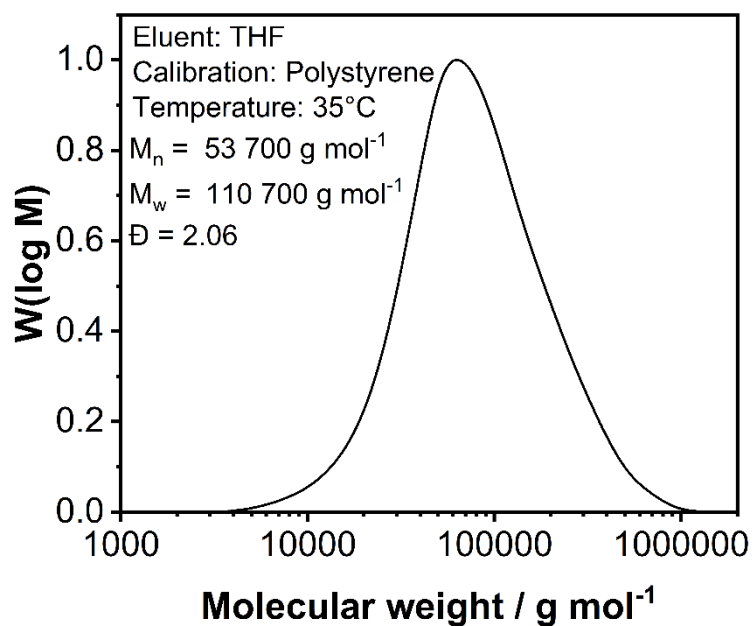


Figure S 4: The GPC curve characterizes the molecular weight distribution of the precursor polymer, providing insight into its polymerization efficiency.

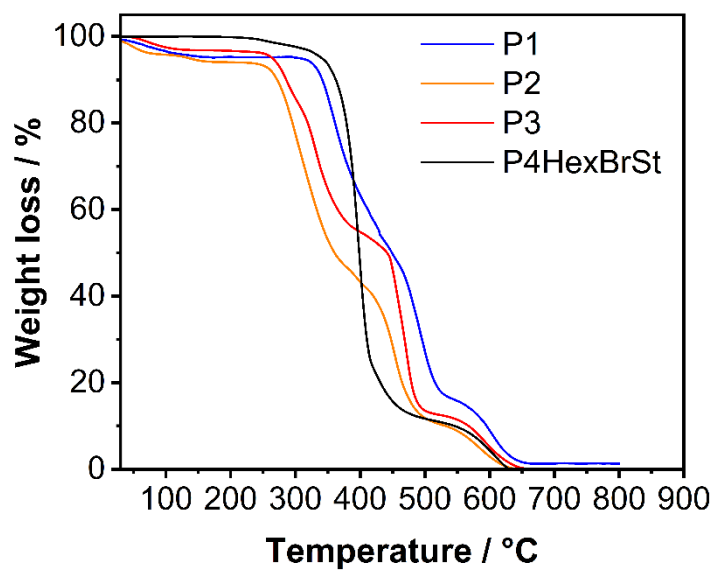


Figure S 5: TGA tracks the thermal stability of the quaternized polymers and the precursor polymer under a synthetic air atmosphere, with a heating rate of 10 K/min, highlighting the degradation temperatures of the materials.

Table S 1: Thermal transitions (Glass transition temperatures,  $T_g$ ) of the precursor polymer P4HexBrSt and the quaternized polymers evaluated on the second heating curve (measured under  $N_2$  atmosphere with a heating rate of  $20 \text{ K min}^{-1}$ ). The TMA-functionalized polymer (P3) did not show a thermal transition in the investigated temperature range.

Polymer	$T_g$ [°C]
P4HexBrSt	-4
P1 (Quin)	112
P2 (Im)	60
P3 (TMA)	-
P4 (Pip)	110

Table S 2: Blend membranes investigated in the present study, with the theoretical IEC ( $IEC_{theo}$ ), the IEC determined via integration of the  $^1H$  NMR spectra ( $IEC_{NMR}$ ) and the IEC's obtained from Mohr's titration ( $IEC_{titrated}$ ) with  $\pm$  one standard variation as error.

Membrane	$IEC_{polymer}$ [mmol g <sup>-1</sup> ]	$IEC_{theo}$ [mmol g <sup>-1</sup> ]	$IEC_{NMR}$ [mmol g <sup>-1</sup> ]	$IEC_{titrated}$ [mmol g <sup>-1</sup> ]
M1 (Quin)	3.17	2.20	2.25	$2.13 \pm 0.07$
M2 (Im)	1.96	1.80	1.76	$1.39 \pm 0.02$
M3 (TMA)	3.80	2.80	2.93	$2.83 \pm 0.04$
M4 (Pip)	3.30	2.40	2.50	$2.35 \pm 0.04$

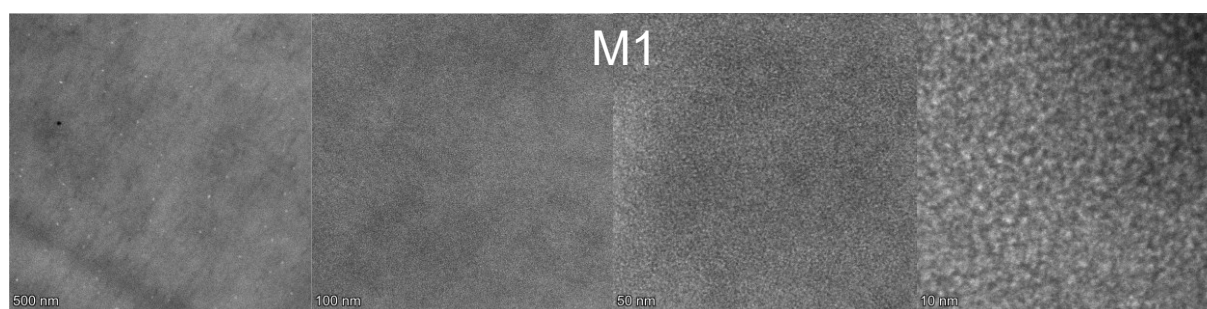


Figure S 6: HAADF-STEM images of M1 with different magnification showcasing a homogeneous membrane microstructure and nanophase separation.

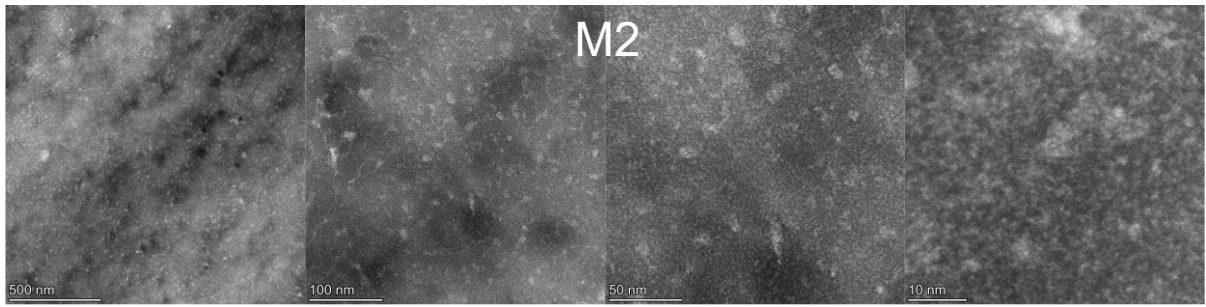


Figure S 7: HAADF-STEM images of M2 with different magnification showcasing a slightly inhomogeneous membrane morphology with agglomerates on a length scale of 15 nm.

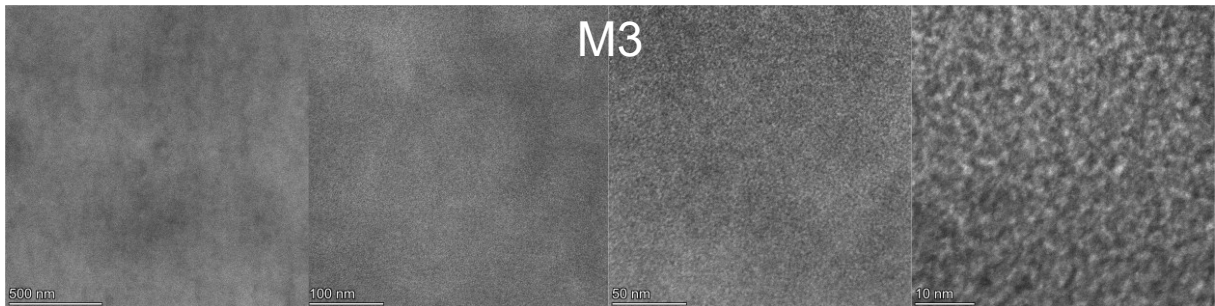


Figure S 8: HAADF-STEM images of M3 with different magnification showcasing a homogeneous membrane microstructure and nanophase separation.

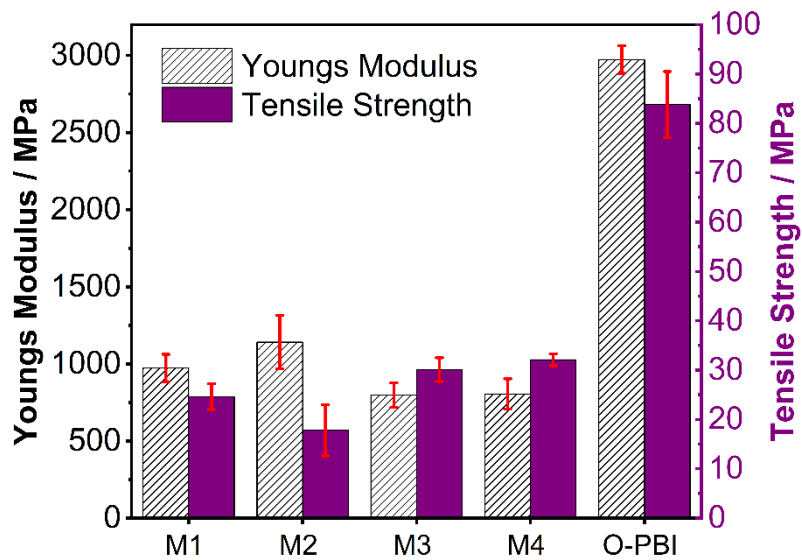


Figure S 9: Tensile properties (Youngs modulus and tensile strength) of the blend membranes M1, M2, M3 and M4 compared to a pure O-PBI membrane.

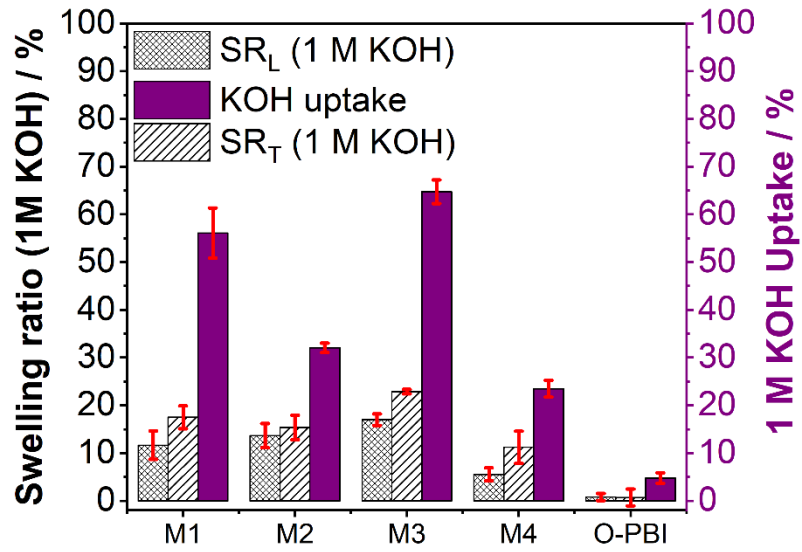


Figure S 10: Dimensional swelling in 1 M KOH (SR<sub>L</sub>: In-plane dimensional swelling, SR<sub>T</sub>: through-plane dimensional swelling) and 1 M KOH uptake of the blend membranes compared to a pure O-PBI membrane.



Figure S 11: Optical images of the blend membranes M1, M2, M3 and M4 highlighting their transparency, homogeneity and absence of precipitates.

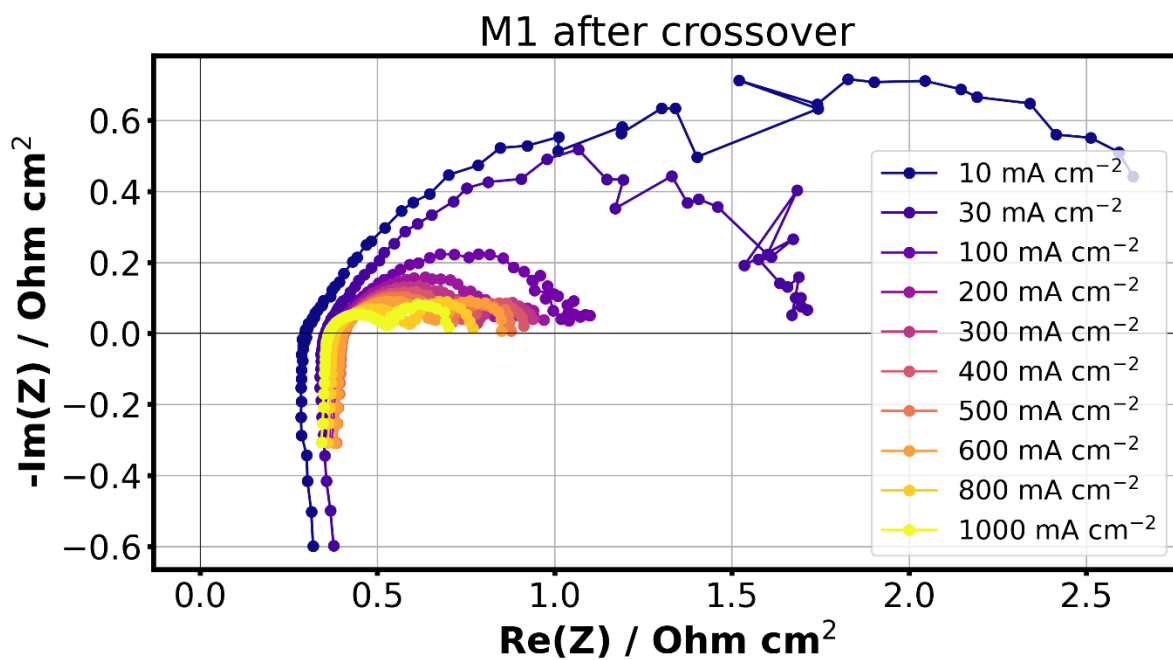


Figure S 12: GEIS (frequency range: 200 mHz to 100 kHz) for M1 at various current densities after the crossover measurement used to extract the high frequency resistance (HFR).

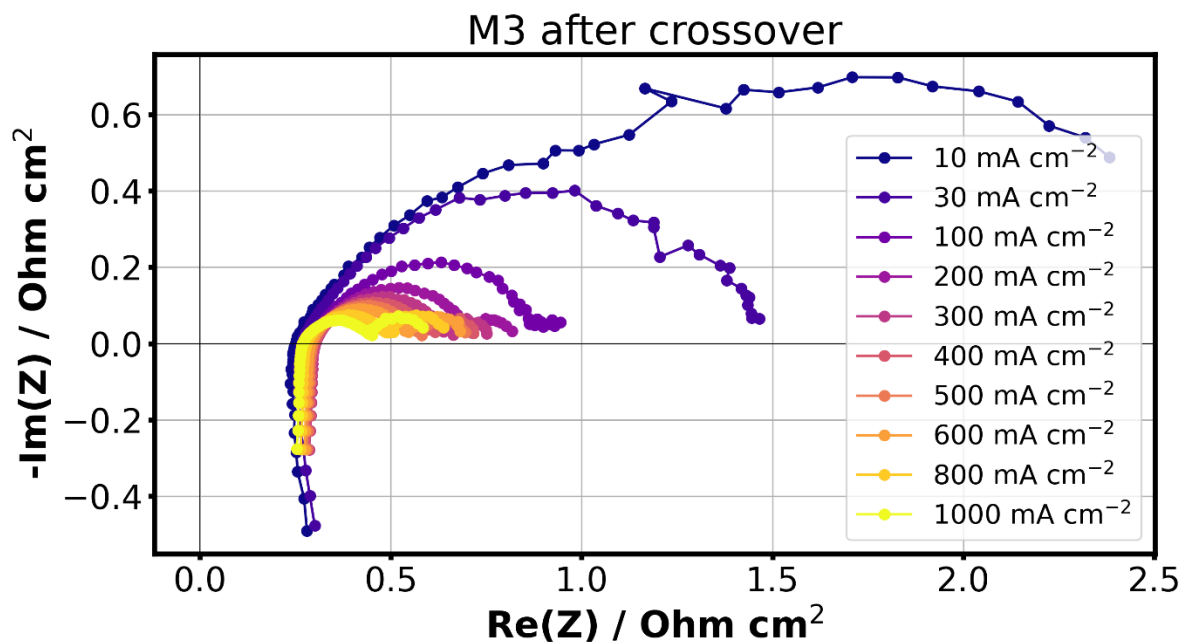


Figure S 13: GEIS (frequency range: 200 mHz to 100 kHz) for the M3 at various current densities after the crossover measurement used to extract the high frequency resistance (HFR).

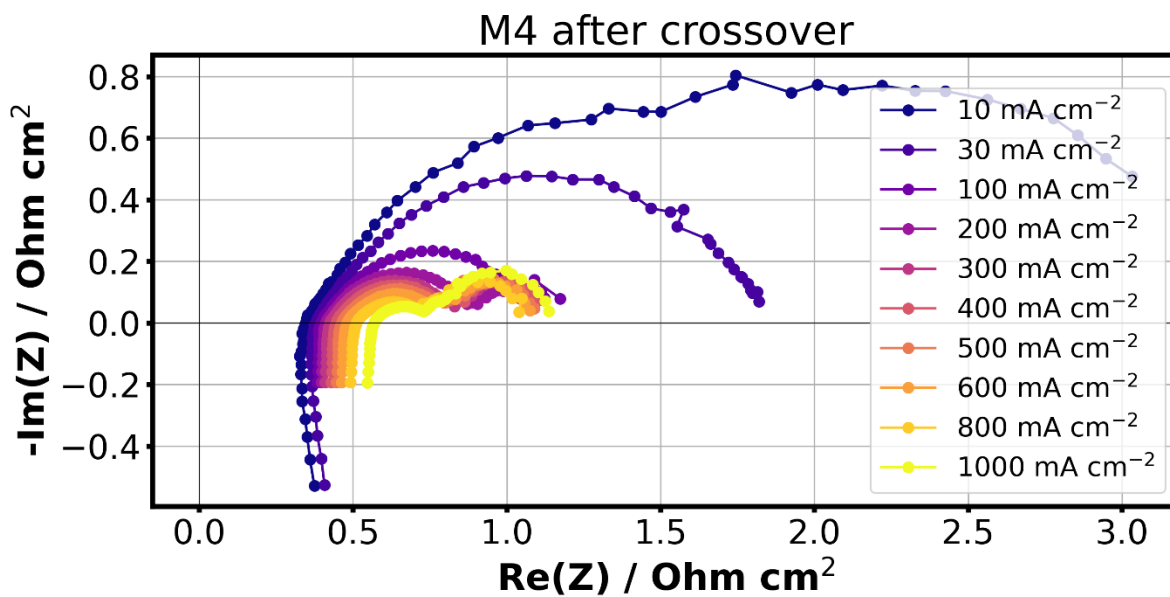


Figure S 14: GEIS (frequency range: 200 mHz to 100 kHz) for the M4 membrane at various current densities after the crossover measurement used to extract the high frequency resistance (HFR).

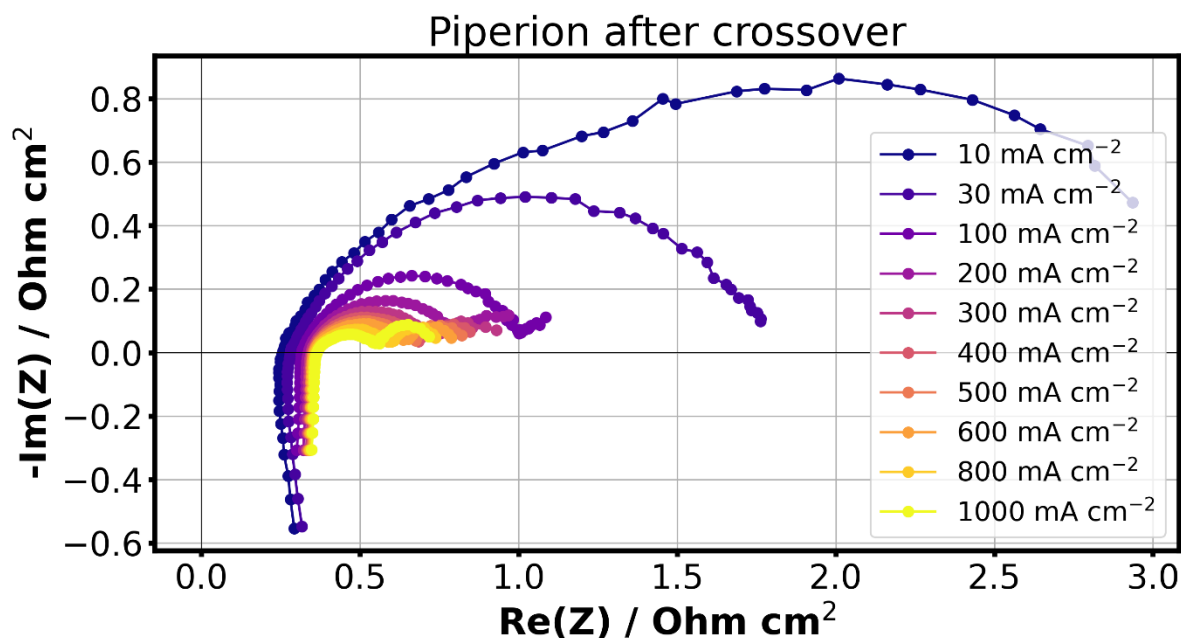


Figure S 15: GEIS (frequency range: 200 mHz to 100 kHz) for the Piperion membrane at various current densities after the crossover measurement used to extract the high frequency resistance (HFR).

The voltage during the crossover measurement was recorded as an initial indicator of membrane durability in AEMWE (Figure S16). All cells underwent a minimum 17-hour crossover test (Figure S16), with testing paused not due to cell failure but due to limited test capacity, requiring the rig to be freed. The HFR comparison before and after the crossover test (Table S3) shows no increase across all membranes, indicating that membrane degradation over the tested time scale is unlikely, as HFR primarily reflects membrane resistance.

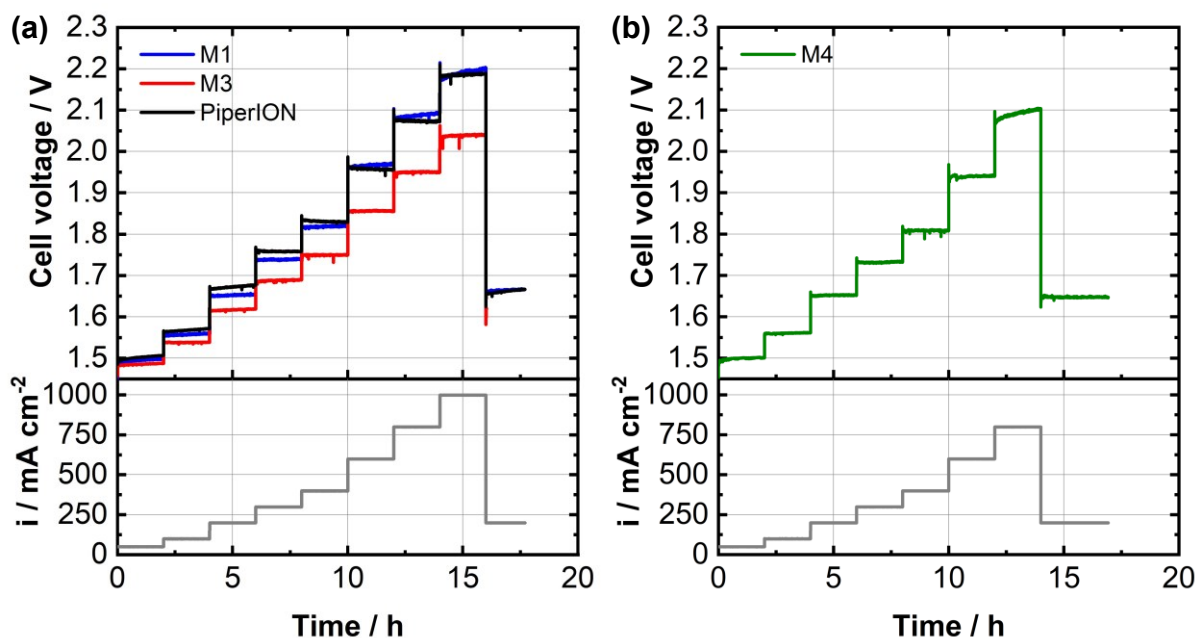


Figure S 16: (a) Cell voltage vs. time during the crossover measurement at different current densities (50, 100, 200, 300, 400, 600, 800 and 1000 mA cm<sup>-2</sup>) for M1, M3 and Piperion vs. time (b) Cell voltage vs. time during the crossover measurement for M4 at varying current densities (50, 100, 200, 300, 400, 600, and 800 mA cm<sup>-2</sup>). The measurement was limited to a maximum current density of 800 mA cm<sup>-2</sup> to ensure the cell voltage remained below 2.3 V, thus preventing potential damage to the electrodes.

Table S 3: High-frequency resistance (HFR) before (BOT) and after (EOT) the crossover test highlighting no significant changes for all membranes.

Membrane	HFR <sub>BOT</sub> @ 10 mA cm <sup>-2</sup> [Ω cm <sup>2</sup> ]	HFR <sub>EOT</sub> @ 10 mA cm <sup>-2</sup> [Ω cm <sup>2</sup> ]
M1	(0.30 ± 0.02)	(0.32 ± 0.04)
M3	(0.27 ± 0.03)	(0.27 ± 0.03)
M4	(0.37 ± 0.02)	(0.34 ± 0.01)
PiperION®	(0.27 ± 0.01)	(0.26 ± 0.01)



- 1 K. M. Hugar, H. A. Kostalik and G. W. Coates, Imidazolium Cations with Exceptional Alkaline Stability: A Systematic Study of Structure-Stability Relationships, *J. Am. Chem. Soc.*, 2015, **137**, 8730–8737.
- 2 L. Hager, M. Hegelheimer, J. Stonawski, A. T. S. Freiberg, C. Jaramillo-Hernández, G. Abellán, A. Hutzler, T. Böhm, S. Thiele and J. Kerres, Novel side chain functionalized polystyrene/O-PBI blends with high alkaline stability for anion exchange membrane water electrolysis (AEMWE), *J. Mater. Chem. A*, 2023, **11**, 22347–22359.
- 3 M. Makrygianni, S. Aivali, Y. Xia, M. R. Kraglund, D. Aili and V. Deimede, Polyisatin derived ion-solvating blend membranes for alkaline water electrolysis, *J. Membr. Sci.*, 2023, **669**, 121331.
- 4 Y. Xia, S. C. Rajappan, D. Serhiichuk, M. R. Kraglund, J. O. Jensen and D. Aili, Poly(vinyl alcohol-co-vinyl acetal) gel electrolytes for alkaline water electrolysis, *J. Membr. Sci.*, 2023, **680**, 121719.